Marek Cięzobka, Edward Lisowski [1)]

UTILIZATION OF METHODS OF ARTIFICIAL INTELLIGENCE FOR DETECTING MANUFACTURING DEFECTS IN HYDRAULIC ELEMENTS

Summary: This paper presents the work conducted in the Institute of Applied Computer Science of Cracov Technical University, related with a novel quality control system for hydraulic elements. Verification of individual objects will take place in the CAD system, which provides the user with selection of desired details, and thanks to implementation of the most modern methods of knowledge engineering, it is also possible to change the monitoring target without introducing any changes in the underlying software. The described application operates in real-time at the production line.
Keywords: quality control system, monitoring, stereovision, 3D virtual map.

INTRODUCTION

In the contemporary world, automation, globalization and unification of standards affected each and every single branch of science and economy. This is possible thanks to transformation of the world around us towards the information society. Computerization of the world, which becomes gradually a global village means that IT systems become increasingly simple in terms of their use and replace in contemporary factories technicians, engineers as well as quality control specialists.

Automated work posts, capable of operating cheaper, often more precisely and commonly under conditions unfavourable to human beings can be also controlled remotely. Through the introduction of the methods of artificial intelligence to routine and scientific analysis in quality control, it is possible to achieve improvement in the results by increasing the measurement precision or calculating additional parameters based of the objects, which cannot be determined by hand, what in turns guarantees better forecast certainty.

This paper presents the work conducted in the Institute of Applied Computer Science of Cracow Technical University, related with a novel quality control system for hydraulic elements. Verification of individual objects will take place in the CAD system, which provides the user with selection of desired details, it is also possible to change the monitoring target without introducing any changes in the underlying software. The described application operates in real-time at the production line.

---

[1] Instytut Informatyki Stosowanej, Wydział Mechaniczny, Politechnika Krakowska.

STRUCTURE AND OPERATION OF THE PROGRAMME

Figure 1 presents the design of a stereoscopic system for quality control of hydraulic valves, comprising appropriately mounted cameras, a computer with the installed software CAD Solid Works Premium 2009 and the elaborated software for detecting defects in the sliding splitters. The initial calibration and rectification of cameras was performed in the off-line mode prior to the process of detection, while the activation procedure, digital image processing and decision on detection operate only in the on-line mode.
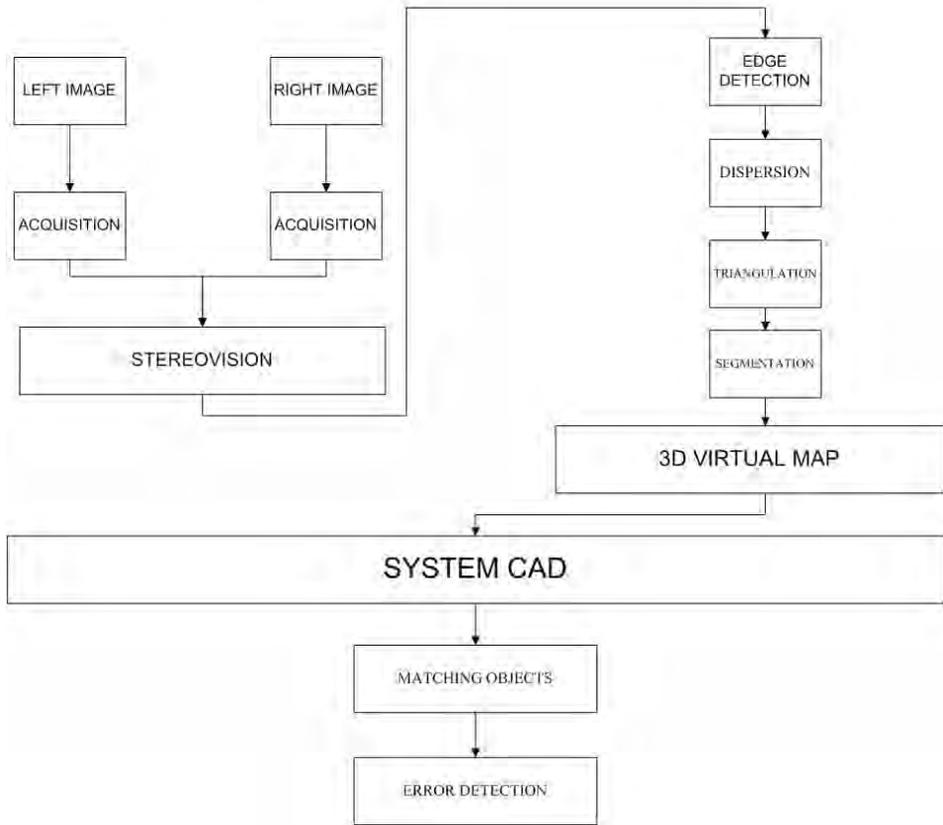

Fig. 1. Block diagram of the system
Rys. 1. Schemat blokowy optycznego systemu kontroli jakości

Image acquisition

Image acquisition, or image capture from an analogue or digital source (video or photographic camera) and delivery of this information to a computer has a critical feature i.e. the obtained discrete image was topologically equivalent to the original continuous image. The described application uses Logitech

QuickCam Connect type cameras, equipped with a VGA resolution converter and an USB interface. These cameras are equipped with an ability of manual adjustment of image sharpness. The functions included in a multi-platform, OpenCV library for image processing were used for capturing images. Images are captured from both cameras simultaneously.

Edge detection

Algorithms of edge detection are subject to continuous research carried out by many scientists, thus their number is rather large. However, the best results are provided by algorithms based on fuzzy sets, even though they need much higher number of computation operations and a single data set in the examined image may need to be processed several times. In this study, we took advantage of a fuzzy logic classifier function presented in the work entitled *„Image edge detection using Fuzzy Classifier"*. This particular algorithm comprises 4 basic steps:

− **step 1:** define the values for three parameters provided by the user i.e. low, high.
− **step 2:** for each pixel, calculate the difference between all 8 surrounding pixels and store them in a vector.
− **step 3:** For each vector, calculate the value of association function, defining the class the given pixel belongs to.
− **step 4:** Based on the principles of fuzzy logic, determine whether the given pixel belongs to the background or an edge.

In order to handle implementation of algorithms used to detect edges, first it is necessary to define several concepts.

Pixel neighbourhood

In the theory of cell automatons, the term "Moore's neighbourhood" or "Moore's surrounding" defines the set of eight cells, which surround the central cell i.e. the set of neighbours comprises all cells which border with the given edge or vertex. The central cell does not make part of its own surrounding. Such a surrounding comprises all neighbouring cells, bordering with edges or vertices.

The first step of this algorithm features calculation of a vector for each pixel in the image (see pixel P5 in the figure):

$$X=[X1, X2, X3, X4, X5, X6, X7, X8],$$

where:

x1 = p1 - p5	x2 = p2 - p5	x3 = p3 - p5	x4 = p4 - p5
x5 = p6 - p5	x6 = p7 - p5	x7 = p8 - p5	x8 = p9 - p5

p1	p2	p3
p4	p5	p6
p7	p8	p9

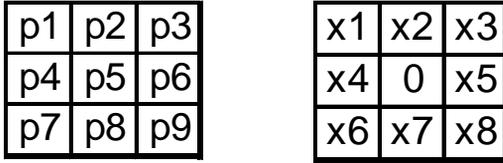| x1	x2	x3
x4	0	x5
x6	x7	x8

Fig. 2. Pixel neighbourhood
Rys. 2. Sąsiadujące piksele

Background and edge class

When vector X for the given examined pixel is already created, next it is necessary to calculate the value of two affiliation functions, describing affiliation to the class of background or the class of edge. Based on the obtained results, it is possible to determine whether the given pixel belongs to an edge or the background. An edge is relatively simple to detect when there are very large differences between the examined pixel and its surrounding. Sometimes, noise can be misinterpreted. Therefore, prior to edge detection, images are filtered to eliminate noise, though there are also algorithms based on fuzzy sets used for noise elimination. e.g. **Competitive Fuzzy Edge Detection**. The value of affiliation functions for the background and edge classes are calculated as follows:

a) background class:

$$\begin{cases} 1 & -> \quad X1 \le L, X2 \le L, ..., X8 \le L \\ Max\{0, 1 - \| X - \mu1 \| 2/\beta & -> \quad wpp \end{cases} \tag{1}$$

b) edge class:

$$\begin{cases} 1 & -> \quad X1 \ge H, X2 \ge H, ..., X8 \ge H \\ Max\{0, 1 - \| X - \mu2 \| 2/\beta & -> \quad wpp \end{cases} \tag{2}$$

It is simple to notice that these functions return a value in the range [0;1]. Classification to the given class is represented in the figure 3.

Calculating the value of a new pixel

When we already have the value of affiliation functions for the aforementioned classes, it is time to take decision whether the given pixel is part of an edge or the background. For that purpose, we use a set of "if ... then" rules, defined as follows:

− **IF** the background affiliation function has a larger value **THEN** change the pixel colour to white,
− **IF** the edge affiliation function has a larger value **THEN** change the pixel colour to black,
− **IF** both affiliation functions have the same value **THEN** change the pixel colour to white [1].
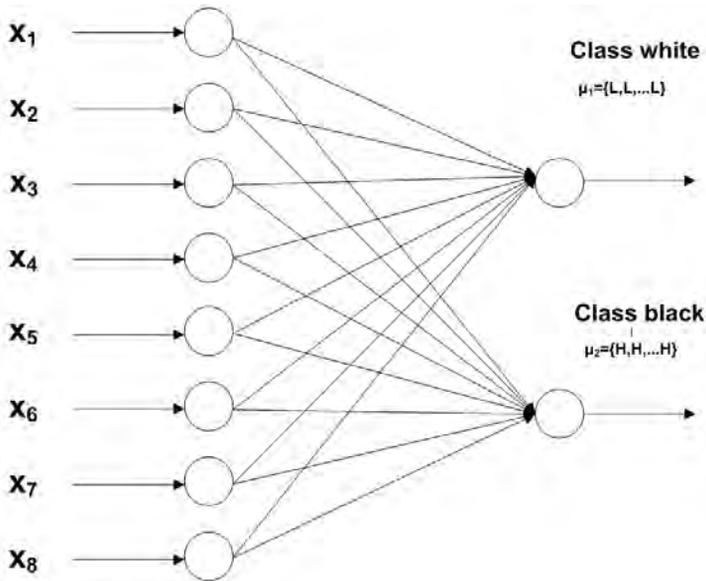
Fig. 3. Edge classification
Rys. 3. Klasyfikacja krawędzi

Result of the algorithm

Figure 4 presents view from the camera in the separator after the edge detection algorithm was executed. The algorithm used in this step will identify the object from the camera and then segment it, which will be then used to create the 3D object.
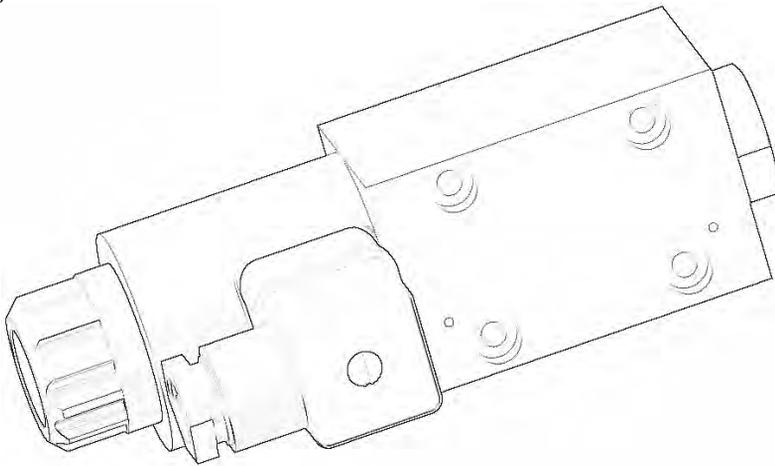

Fig. 4. Examined separator after the edge detection
Rys. 4. Badany separator po detekcji krawędzi

Epipolar geometry

Utilization of the epipolar geometry is a critical requirement of the stereo-visual system. Figure 5 presents two perspective cameras, including their projection midpoints: O_l , O_r and image planes: p_l , p_r . The focal length is equal to : f_l i f_r, respectively. Each camera is located in its own reference system, the centre of which is located in the projection midpoint and the Z axis is the optical axis. Vectors $P_l = [X_l, Y_l, Z_l]$ and $P_r = [X_r, Y_r, Z_r]$ refer to the same point in the space P, which may be treated as a vector existing in the right and left reference system of cameras, respectively. Vectors $p_l = [x_l, y_l, z_l]$ and $p_r = [x_r, y_r, z_r]$ correspond to projections P to left and right image plane, respectively - and are expressed in the appropriate reference system. For all the image points, it is always true that: $z_l = f_l$ lub $z_r = f_r$.
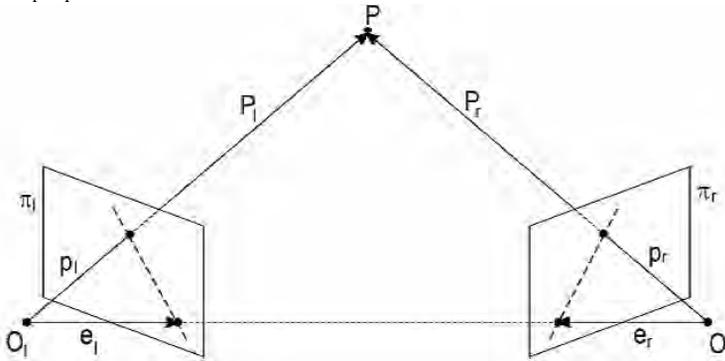

Fig. 5. Epipolar geometry
Rys. 5. Geometria epipolarna

The reference systems of the left and right cameras are interconnected using external parameters of a stereo-visual system. They define a fixed transformation in the 3D space using a translation vector $T = (O_r – O_l)$ and a rotation matrix R. For point P, it is possible to determine relations between P_l and P_r : $P_r = R(P_l - T)$.

For the given stereo-visual system, any point P in 3D space defines the plane π_p, traversing through P and the projection mid-points for both cameras (see Figure 5). Plane π_p is referred to as the epipolar plane, while intersections of the plane π_p with the planes of both images are referred to as coupled epipolar lines. Image of the projection midpoint of the second camera in the first camera is referred to as the epipolar midpoint. Only one epipolar line passes through each point on the image, excluding the epipolar midpoint. All epipolar lines of the given camera pass through its epipolar centre. The primary assumption of the epipolarity states that corresponding images must be located on coupled epipolar lines [2].

Dispersion

Stereovision is based on dispersion, i.e. the distance between images of the same point in the planes of both cameras. A smaller dispersion indicates in reality a smaller distance between the given object from the camera system. In the aforementioned case, it is visible that the upper cube is much further than the bottom one.

During the process of creating a sparse dispersion map, each stereo-couple must pass through three stages of processing i.e.:

− detection of characteristic points, for which the depth value will be calculated, e.g. edges,
− adjusting equivalents,
− reconstruction of the 3D space coordinates.

The calculated dispersion for each point in the 3D scene creates the so-called dense dispersion map. The process of automated determination of the dense dispersion map in real time for a pair of images was supported by an image alignment algorithm. In this algorithm areas with specific, pre-defined areas are aligned. The most commonly used measure of similarity between a pixel in the reference image and a pixel in the other image is the SAD (Sum of Absolute Differences). For coloured images, the SAD measure is described using the following formula:

$$SAD(x_R, y_R, d) = \sum_{i=\frac{1}{2}(winx-1)}^{\frac{1}{2}(winx-1)} \sum_{j=\frac{1}{2}(winx-1)}^{\frac{1}{2}(winx-1)} [|R_R(x_R+i, y_R+j) - R_L(x_L+i, y_L+j)| +$$
$$+ |G_R(x_R+i, y_R+j) - G_L(x_L+i, y_L+j)| +$$
$$+ |B_R(x_R+i, y_R+j) - b_L(x_L+i, y_L+j)|] \tag{3}$$

The SAD measure is calculated for each point in the reference image in the given dispersion range (offset) d i.e. SAD values (x_R, y, d) are stored in a three-dimensional table, the so-called dispersion space map, with the dimensions of $(w+winx+1) \times (d_{max}-d_{min}+1) \times (h+1)$. In order to calculate subsequent SAD, a "shifting window" technique was used in the algorithm. Searching for reliable minimum values of the SAD measure is performed in four steps, by finding the global minimum SAD_{min} and three smallest values $SAD_1 < SAD_2 < SAD_3$ [3].

Triangulation

All points obtained from the dispersion map create a triangle mesh; it was created using the algorithm proposed by Wang D., Hassan O., Morgan K., Weatherill N. using the Delaunay triangulation method. This particular type of triangulation works by combining individual points into triangles in such a way that no

points can be found within the circle circumscribed on any of the triangles constructed during the process of triangulation [4].

This algorithm of mesh construction allows for complete automation of any area, no matter what level of its complication, as well as simple introduction of many adaptive methods. One of the primary properties of the Delaunay triangulation process is the fact that the generated triangles are as close to equilateral triangles as possible - this particular property is especially valuable in the methods of finite elements.

A generic algorithm for triangulation using the Delaunay method is as follows:
− generate initial points,
− triangulate the hull of the initial point could,
− find the edge of the area and eliminate triangles located outside of this area,
− generate (as needed) internal nodes and introduce them to the triangulation,
− improve the quality of the obtained mesh (mesh adaptation),

Shepard interpolation

The measurement results in a set of points, which do not (typically) generate a regular node mesh. If there was a way to convert this point cloud into a regular mesh, it would substantially simplify its further analysis and potential transformations [5]. For this purpose, Shepard interpolation was used, which is an extension to the classic Newton interpolation to more than one dimension:

$$f(x,y) = \frac{\sum_{i=1}^{N} w_i(x_i, y_i) \cdot z_i}{\sum_{i=1}^{N} w_i(x_i, y_i)} \tag{4}$$

where:

$$w_i(x_i, y_i) = \frac{1}{(\sqrt{(x - x_i)^2 + (y - y_i)^2})^n} \tag{5}$$

Segmentation

In the application, a hybrid segmentation algorithm was used, utilizing edge detection techniques and random Markov fields. 3D scene segmentation algorithm executes detection of individual planes and 'obstacles', i.e. objects which do not meet the plane equation, in an iterative mode. The searching process is executed on a point grid with the TIN structure, in the interval of 16 pixels. Image segmentation is based on classification of individual triangles based on two image colour

164

components i.e. RN and BN, normalized in order to eliminate the influence of local changes in the intensity of external lighting. The process of segmentation results in a table (so-called segmentation map), the elements of which store indices of colour classes to which individual pixels of the examined image were assigned to.

Random Markov Field

Random Markov field are used in image analysis for various purposes, including among the others analysis of texture, image synthesis, image restoration, classification, segmentations and surface reconstruction.

Arbitrary systems with spatial interaction are described using statistical approach in the publications of J. Besaga. It describes an Bayesian image analysis approach, and in particular a priori probability distributions, based on a naive Bayer classifier. Morphological random Markov fields are especially applicable for formulation of a priori probability models, which are used in this analysis.

The primary task of the Bayesian analysis is focused on recovery of image based on existing data records. Examples of other tasks of such analysis include:

− classification: For example, let's assume that records Y have the form of satellite images taken at several various wavelengths. In this case, the image may represent the observed region into specific fields, including among the others crops, vegetables, gardens, forest plots etc.

− segmentation. In this case, specific records Y may have the form of greyscale images, representing a particular scene, while a map of edges for objects present in this scene.

− motion detection.

In the examination, a model was used in which each pixel can have a value of 0 or 1 (generalized Ising model) [6].

MATCHING OBJECTS

Once all the aforementioned algorithms have been executed, the scanned 3D model of the project is obtained, which is then imported to the CAD system. In the next step, it is necessary to adapt the planes to the CAD model. In the application, the previously identified edges were used in combination with the Levenberg–Marquardt algorithm. In this particular case, using the model developed in the CAD system by designers: $(x_i, y_i, z_i) \in R^3$, where $i = 1,2,3...,N$ we are looking for match $y' = f(x,y,z)$ from the set created in the result of stereo-vision.

The Levenberg-Marquardt algorithm can find the solution of the non-linear function optimization task, which can be described in the following form:

$$\Phi(x) = \frac{1}{2}\sum_{i=1}^{N} r_i^2(x) \tag{6}$$

where $x \in \mathbf{R^n}$ and $N \geq n$. To simplify the problem, we represent the function r_i as a vector $r\ (x) = (r_1(x),...,r_N(x))$ (referred to as a *residual vector*).

This is achieved thanks to the iterative algorithm, with the step equal to:

$$x_{i+1} = x_i - (H(x_i) + \lambda \text{diag}[H])^{-1} \nabla \Phi(x_i) \tag{7}$$

where:

$$\text{diag}[H] = \begin{bmatrix} h_{11} & 0 & .. & .. & 0 \\ 0 & h_{22} & . & . & 0 \\ . & . & . & . & . \\ . & . & . & . & . \\ 0 & 0 & .. & .. & h_{nn} \end{bmatrix} \tag{8}$$

$H(x_i)$ it is Hessian for the function $\Phi(x_i)$. The algorithm in its step-wise form can be described as follows:

− calculate value x_{i+1} based on x_i and equation (7),
− calculate the error value in this point x_{i+1},
− if the error value increased, return to value x_i , increase the factor λ *k*-times and return to step 1 (linear approximation of the minimized function in the surrounding x_i turned out to be inaccurate, thus it is necessary to increase the "influence" of the largest slope method),
− if the error value decreased, accept this step and decrease the factor λ *k* -times (assumption of the linear character of the minimized function in the surrounding x_i turned out to be sufficiently precise, hence it is necessary to increase the "influence" of the Gauss-Newton method) [7].

Figure 6 presents the model after the 3D reconstruction is completed.

Fig. 6. Model after reconstruction
Rys. 6. Model po rekonstruk-cji 3D

COMPARISON OF MODELS

Models are compared automatically in the CAD system, thanks to the use of API and the fact that Solid Works provided .NET and COM references. In the system, objects can be compared in many ways, including among the others:
- global and directional surface comparison,
- intersection comparison,
- edge comparison,
- comparison of local curvature of the point cloud and triangle mesh,
- comparison of element features,
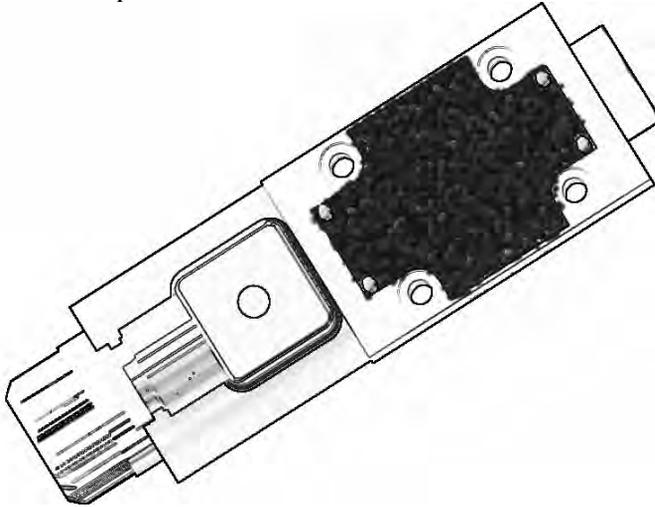- occurrence of specific elements.

Fig. 7. Result of the system operation
Rys. 7. Rezultat operacji porównywania modeli

Figure 7 presents the effects of comparison between the reconstructed model and the data set stored in the data base by designers. Based on the examined figure, it is clear what elements are missing, though the system automatically calculates points and stores them in a table (just like Table 1). In this particular case, it is part6.

Table 1. Comparison between the reconstructed model and the data set stored in the data base

Tabela 1. Wykaz różnic między rekonstrukcją modelu a opisującą go bazą danych

part	number of differences	part	number of differences
part1	2	part7	12
part2	31	part8	12
part3	2	part9	33
part4	45	part10	21
part5	23	part11	23
part6	**1863**	part12	12

CONCLUSIONS

The described system, together with the whole investigation equipment represents an innovative system for analysis of manufacturing errors in hydraulic elements. The system is effective, fast and complex, taking advantage of the latest IT technologies and at the same time very functional. Utilization of this application eliminates the need for human inspection.

The system can be also expanded and utilized in other branches of the industry. Manufacturing errors are classifies as so-called gross errors (lack of parts, screws etc.) - the system was not tested for precise quality control.

REFERENCES

1. Liang L. R., Looney C. G.: Competitive fuzzy edge detection, Applied Soft Computing 3 , 2003.
2. Hartley R., Zisserman A.: Multiple View Geometry in Computer Visio Second Edition, Cambridge University Press, 2004.
3. Vassiliadis S., Hakkennes E. A., Wong J. S. S. M., Pechanek G. G.: The Sum-Absolute-   Difference Motion Estimator Accelerator, in Proceedings of the 28th EUROMICRO Conference, pp. 183-188, Dortmund, Germany, September 2002.
4. Wang D., Hassan O., Morgan K., Weartherill N.: Efficient surface reconstruction from contours base on two-dimensional Delaunay triangulation. International Journal of Numerical Methods in Engineering 2006, 65, 5, 734-751.
5. Kordecki A., Bal A.:, Wpływ wyboru pól wzorca na wierność odwzorowania barw w procesie kalibracji kolorymetrycznej, Materiały 6. Konferencji Naukowej „Informatyka – Sztuka czy Rzemiosło” KNWS'09 Rydzyna, 3-5 czerwca 2009.
6. Wirjadi O.:, Survey of 3d image segmentation methods. Fraunhofer-Institut für Techno- und Wirtschaftsmathematik ITWM 2007.
7. Gill P. E., Murray W.: Algorithms for the solution of the nonlinear least-squares problem, SIAM Journal on Numerical Analysis, 1978.

WYKORZYSTANIE METOD SZTUCZNEJ INTELIGENCJI DO WYKRYWANIA BŁĘDÓW PODCZAS WYTWARZANIA ELEMENTÓW HYDRAULICZNYCH

Streszczenie: W artykule przedstawiono prace prowadzone w Instytucie Informatyki Stosowanej Politechniki Krakowskiej, związanych z nowym systemem sterowania jakością przy wytwarzaniu elementów hydraulicznych.
Weryfikacja poszczególnych obiektów odbywa się w systemie CAD, który umożliwia użytkownikowi wybór żądanych elementów, a dzięki wdrażaniu najnowocześniejszych metod zarządzania danymi, możliwa jest także zmiana obiektu monitorowania, bez konieczności wprowadzania żadnych zmian w podstawowe oprogramowanie. Przedstawiona w artykule aplikacja działa w czasie rzeczywistym na linii produkcyjnej.
Słowa kluczowe: system kontroli jakości, monitorowanie, stereowizja, trójwymiarowa mapa wirtualna.